MACROSCOPIC MODELING OF THE MICROSTRUCTURAL EVOLUTION IN CASTINGS USING THERMODYNAMIC FORMULATED PHASE DIAGRAMS

K. Greven, M. Fackeldey, A. Ludwig, T. Kraft*, M. Rettenmayr*, P. R. Sahm

Giesserei-Institut, RWTH Aachen
Intzestrasse 5, D-52056 Aachen, Germany
Tel: +49-241-80-4067, Fax: +49-241-8888-276, e-mail: klaus.greven@gi.rwth-aachen.de

*Technische Universität Darmstadt,
Petersenstrasse 27, D-64287 Darmstadt, Germany

Abstract

Mechanical properties of castings are dependent on their microstructure, e.g. dendrite arm spacing. To improve the prediction of the microstructural evolution in cast parts, an approach is presented which couples a microscopic model, a macroscopic model and a programmable interface for calculating thermodynamic equilibria. The macroscopic calculations were performed by means of the in-house 3D-FEM-program CASTS. It permits the simulation of the temperature distribution during solidification for complex shaped castings. The micro model predicts the dendritic solidification of ternary alloys using a plate model. It characterizes important microstructural features such as dendrite arm spacing and the amount of eutectic fraction. Effects such as solid state back diffusion, dendrite arm coarsening and tip undercooling are considered. Phase diagram information for the multi-component system is provided on-line by ChemApp™. Both the macro and micro calculation are fully coupled via the release of latent heat at each node of the finite element mesh. Permanent mold casting experiments with different ternary aluminum alloys are performed to validate the complex simulation.

Modeling of Casting, Welding and Advanced
Solidification Processes VIII
Edited by B.G. Thomas and C. Beckermann
The Minerals, Metals & Materials Society, 1998

Introduction

Nowadays, numerical investigations of casting processes can be performed on both the macroscopic and microscopic level, but most common (especially for industrial applications) are still simulations on the macro level. They allow the global prediction of mold filling, solidification and stress formation. A rough estimation of the microstructure can be made e.g. by means of criterion functions [1]. Many numerical techniques on the micro level have also been developed to predict the local evolution of microstructure and the formation of microsegregation as a function of the global cooling conditions. Recent reviews of analytical, semi-empirical and numerical methods can be found in [2, 3]. The most advanced models take into account various effects such as solid state diffusion, dendrite arm coarsening and undercooling. As demonstrated by Boettinger et al. [4, 5], the on-line use of thermodynamic programs is advisable to enhance the accuracy of thermodynamic data for multi-component alloys. Micro and macro models should ideally be strongly coupled to take into account mutual influences between microstructural evolution and temperature changes. This paper presents such a fully two-way coupled modeling. The goal is to develop a general three-dimensional method of simulation which is not restricted to certain alloy systems.

Method of Simulation

A. Macro Model

The described simulations on the macro level are performed by means of the in-house package CASTS, a 3D finite element code. Detailed descriptions and application examples can be found in [6-8]. The mesh can be generated with the commercial software IDEAS-supertab™. To realize the interfacial heat flow, additional elements are enmeshed between different materials. After defining temperature-dependent thermophysical properties and setting appropriate initial (e.g. pouring temperature) and boundary conditions (convection, insulation and radiation including view factors) all information is stored in a command file. During the mainprocessing the program calculates the temperature evolution iteratively, taking into account the release of latent heat, which is evaluated by the micro model.

B. Micro Model

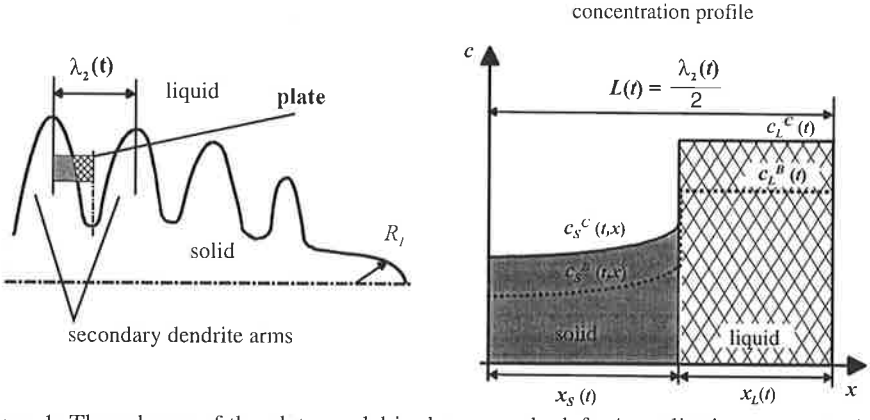

Figure 1: The scheme of the plate model is shown on the left. A qualitative concentration profile of both alloy components *B* and *C* is depicted on the right.

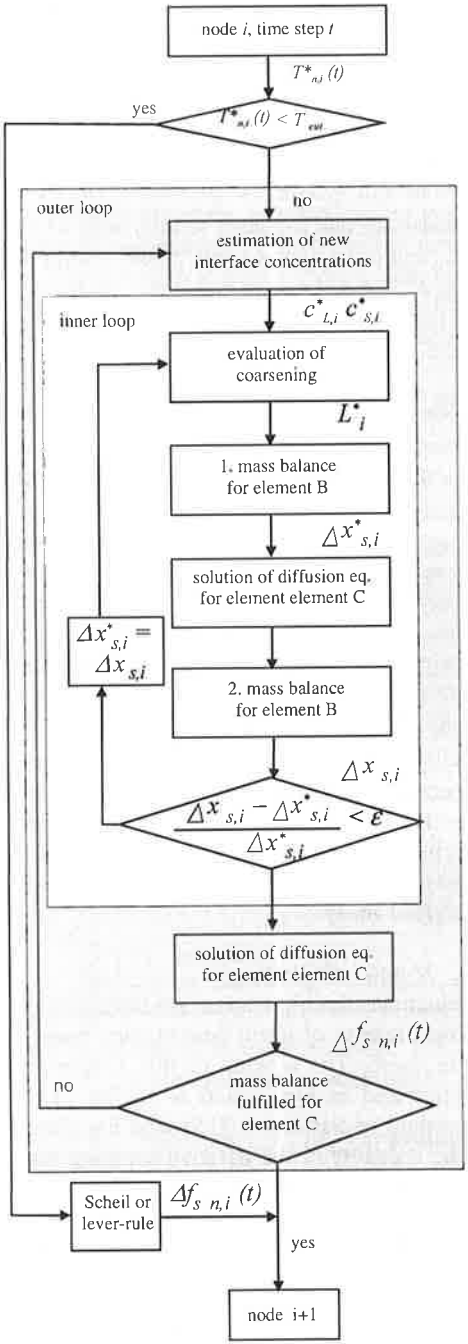

Figure 2: Flowchart of the micro model (n: number of iterations).

The microsegregation model predicts primary dendrite trunk spacing, secondary dendrite arm spacing and phase amounts based on an approach of Róosz and Exner [9] where the complex dendritic structure is approximated by a plate morphology (see Fig. 1). Although this poor approximation of a part of a dendrite, it has been shown that this model yields good agreement between calculation and measurement [9-12]. Coarsening is calculated by the semi-empirical power-cube equation for the time evolution of λ_2 [9]. Complete mixing is assumed in the liquid and the volume element is thought to be at a uniform temperature T. All information concerning the phase diagram was calculated with the aid of the programmable thermodynamic calculation interface ChemApp™ .It consists of a library of FORTRAN subroutines that allow the calculation of thermodynamic equilibria by minimizing the Gibbs free energy. The definition of the thermodynamic equilibrium in combination with the thermodynamic data file of the concerned system serves as an input for ChemApp™. As a result it returns the equilibrium values of various quantities, e.g. temperature, amounts of phases, phase compositions, thermodynamic potentials, heat capacity etc.

The concentration profiles of the alloying elements B and C in the solid are calculated by a fully implicit FD scheme. To ensure the fulfillment of the mass balance during the simulation two iteration loops are necessary. The resulting scheme is shown in Fig. 2.

I. The interfacial concentration value of element B in the liquid c_L^{B*} of the preceding time step remains unchanged, which allows the calculation of $c_S^{B*}, c_L^{C*}, c_S^{C*}$.

II. In the inner iteration loop the advance of the solidification front is calculated iteratively using the mass

balance for element C and solving the respective diffusion equation.

III. After the convergence of this loop, the diffusion equation for B is solved and the second mass balance is proved. If it is not fulfilled within a given error limit, the procedure is resumed again in I with a new value of c_L^{B*}.

In both iteration loops the method of Anderson/Björck [13] is used. The resulting solid fraction f_s is calculated as the ratio $x_s(t)/L(t)$ (see Fig. 1). In the eutectic groove, the growth of primary α-dendrites is assumed to be completed while the secondary α- and β-phases solidify with a Gulliver-Scheil like behavior. This implies a disperse distribution of both eutectic phases within the remaining melt. The undercooling of the dendrite tip ΔT^*, consisting of curvature, solutal and gradient undercoolings, is calculated on the basis of the KGT-model and considered in the micro-model by applying a truncated lever-approximation.

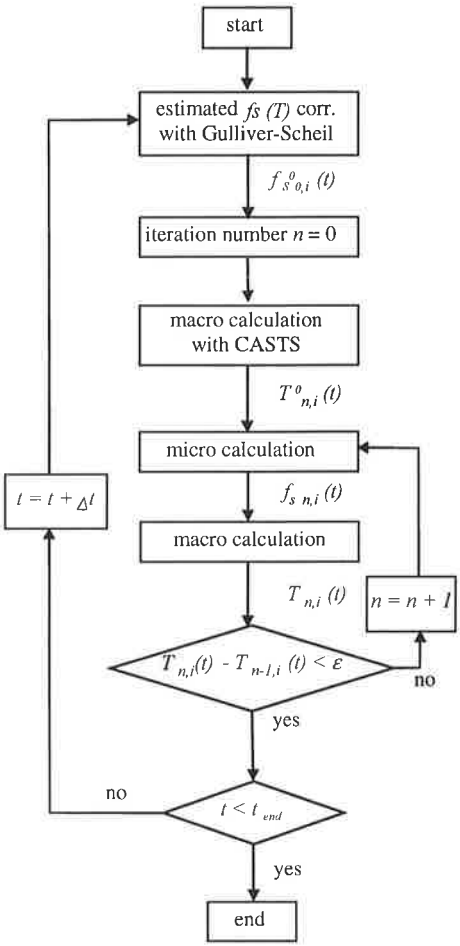

Figure 3: Scheme of the fully coupled modeling

The thermal gradient G and the solidification velocity $V (= \dot{T} / G)$, which are needed in the KGT-model, are taken at each FEM-node at T_L from a conventional macro-calculation (latent heat release due to Gulliver-Scheil), performed in advance. Undercooling of the binary and ternary eutectic has been neglected. The primary spacing is calculated using the approximate equation given in [14]. In this equation one has to specify ΔT, R and G. ΔT is taken as the difference between T_L - ΔT^* and the temperature where the calculated solidification path enters the eutectic groove. The dendrite tip radius R is calculated from the KGT-model and G is approximated as described above.

C. Method of Coupling

Micro and macro program are linked via the local release of latent heat at each node of the mesh. The scheme of this coupling is illustrated in Fig. 3 and is similar to the method of Sasikumar [15] who has shown the necessity of the iterative coupling for a simple case. At the beginning of each time step t the iteration loop starts with an estimated fraction solid (f_s) for all nodes i. It determines the release of latent heat from the macro calculation. With this evaluated temperature distribution $T^{0}_{n,i}(t)$ the micro model simulates the microstructural evolution, leading to a better approximation of f_s which is again input for a repeated macro

calculation. This procedure is repeated until sufficient correlation between the temperature distribution of the actual and previous iteration is obtained.

Experimental Investigations

In order to validate the described course of procedure a step wedge was cast in a permanent mold. Several casting experiments were performed with different AlCuSi-alloys, table I. The outer dimensions of the selected casting system are shown in Fig. 4. This experimental setup permits the observation of both fine and coarse microstructures due to different cooling conditions. Furthermore, it allows reproducible results. The rectangles in Fig. 4 reveal the positions of the samples where microstructural measurements were taken. Furthermore thermocouples were installed at ten positions to monitor solidification. The pouring temperature was 700 °C.

Table I: Composition of the three different AlCuSi-alloys used for the test castings.

	Alloy 1	Alloy 2	Alloy 3
C_{Cu} [wt.%]	5.0	2.0	5.0
C_{Si} [wt.%]	5.0	5.0	2.0

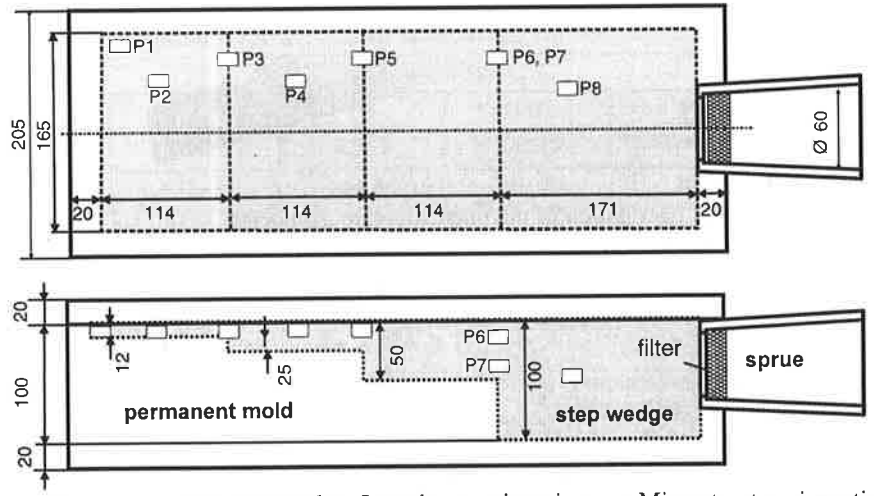

Figure 4: Geometry of the step wedge. Lengths are given in mm. Microstructure investigation was performed at the positions P1 - P8.

Results and Discussion

Figure 5 shows the calculated microstructure parameters λ_1 and λ_2 for an AlCu5wt.%Si5wt.% alloy. Because of the symmetry of the problem, only one half of the cast part was simulated. The FEM-net contains 1276 nodes including the mold. 340 nodes are needed for the step wedge. As expected, in the parts of the step wedge solidifying at large velocities, i.e. the thinner steps or the corners of the four steps, a fine microstructure develops, whereas in the thick step a coarse microstructure occurs. This behavior is also reflected in Fig. 6, showing three micrographs taken from different steps of the casting. It turned out to be very difficult to identify and measure the volume fraction of the different phases, especially to distinguish between binary and ternary eutectic. Thus there are no experimental values for the ternary eutectic fraction f_e. Presently we are working on the development of an adequate metallurgical method which en-

ables the measurement of f_e. Therefore the comparison between simulation and experiment is still reduced to the values of the dendrite trunk and dendrite arm spacing.

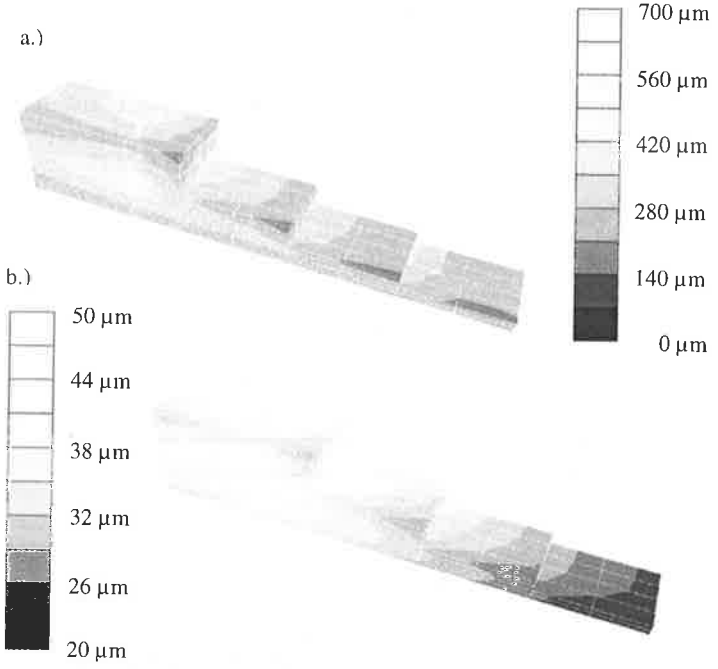

Figure 5: The simulated distribution of the microstructure parameters λ_1 (a.) and λ_2 (b.) for an AlCu5wt.%Si5wt.% alloy.

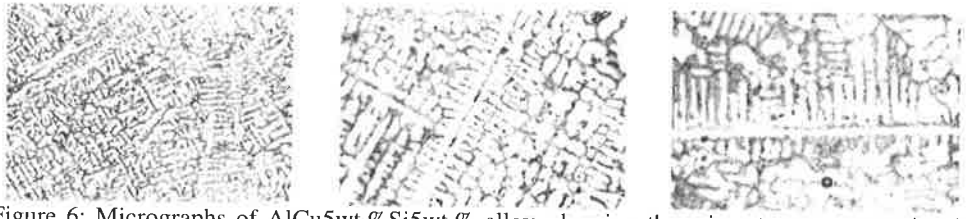

Figure 6: Micrographs of AlCu5wt.%Si5wt.% alloy, showing the microstructure occurring in different steps of the casting (positions P3, P5, P6 (see Fig 4)).

Table II shows the comparison of experimental and simulated values for different samples. It is obvious that the simulation shows good agreement with the experimental values for the dendrite arm spacing λ_2. The reasons for the disagreement in the dendrite trunk spacing λ_1 are as follows. The expression used for the calculation of λ_1 considers a simplified geometry of the dendritic morphology for directional solidification. In our experiments, however, only partial columnar growth occurs. Further, the used expression is valid only for steady state solidification. Therefore the simulated dendrite trunk spacing can only be interpreted as a rough estimation of the order of magnitude.

As expected, the consideration of dendrite tip undercooling has no decisive influence on the results of the simulation for the considered experimental situation. The values of the dendrite arm and trunk spacing are reduced by not more than about 5 to 10 %.

Table II: Comparison of the simulated and the experimentally measured microstructure parameters λ_1 and λ_2 in µm.

a.) Dendrite arm spacing (λ_2):

AlCu5wt.%Si5wt.%								
Position	P1	P2	P3	P4	P5	P6	P7	P8
Sim.	14.75	16.63	16.72	22.41	22.95	27.85	26.17	31.62
Exp.	14.67	15.12	16.82	24.07	29.09	33.29	29.75	34.72
AlCu5wt.%Si2wt.%								
Position	P1	P2	P3	P4	P5	P6	P7	P8
Sim.	22.07	24.18	25.13	33.07	34.11	41.67	35.28	46.61
Exp.	25.07	16.93	20.58	32.68	29.36	43.09	31.94	37.70
AlCu2wt.%Si5wt.%								
Position	P1	P2	P3	P4	P5	P6	P7	P8
Sim.	15.20	17.21	17.52	23.11	23.76	28.25	27.02	32.38
Exp.	13.01	19.75	-	24.62	-	-	-	-

b.) Dendrite trunk spacing (λ_1):

AlCu5wt.%Si5wt.%					
Position	P4	P5	P6	P7	P8
Sim.	180.70	217.7	220.79	274.16	128.07
Exp.	133.00	164.30	289.70	225.00	136.20

The simulations was run on a SGI™ work station with R10000 processor using about 20 h CPU time. A conventional simulation of the respective simulation, which means estimating $f_s(T)$ with Gulliver-Scheil and no microstructure simulation, takes about 0.5 h CPU time. The main reason for the long computation time is that two iteration loops are necessary in the micro program. With a more sophisticated method of iteration or parallel computation on different processors the necessary computation time might be drastically reduced.

Conclusion and Outlook

A full coupling of a 3D-macro model with a micro model was used to simulate the microstructural development during solidification. A thermodynamic calculation interface was used to calculate the phase diagram information. The results show good agreement with the experiment for the dendrite arm spacing λ_2. The expression used for the calculation of λ_1 turned out to be unsuitable for the description of the experiments. The shown method of simulation is quite complex, but with the increasing computational capacities the needed computation time will be drastically reduced. Furthermore the on-line calculation of thermodynamic phase equilibria can easily be applied to different alloy systems.

In ongoing studies an improved model for the calculation of the primary spacing λ_1 of the dendrites will be implemented and an experimental procedure for the determination of f_e developed. Furthermore, a more complex treatment for the solidification in the eutectic groove could be used if there is a deeper insight in the multiphase solidification of the respective alloy. Effects such as solute trapping or the consideration of kinetic and eutectic undercooling can easily

be implemented. Finally a more sophisticated iteration method will be used to reduce the computation time to allow the simulation of more complex geometries.

Acknowledgments

This work was done with financial support of the DFG (SFB 370 "Integrative Werkstoffmodellierung", Graduiertenkolleg "Schmelze, Erstarrung, Grenzfläche") for which the authors are very grateful.

References

1. P.R. Sahm, P.N. Hansen, Numerical Simulation and Modeling of Casting Processes for Foundry and Cast-House (Zürich, Int. Committee of Technical Foundry Association CIATF 1984)
2. M. Rappaz, "Modelling of Microstructure Formation in Solidification Processes", Int. Mater. Rev. 34 (1989), 93-123.
3. T. Kraft, H.E. Exner, "Numerische Simulation der Erstarrung - Teil 1+2", Z. Metallkd. 87 No. 8 (1996), 598-611 and 652-660.
4. W.J. Boettinger et al. "Development of Multicomponent Solidification Micromodels Using a Thermodynamic Phase Diagram Data Base", in Proc. of Int. Conf. Modeling of Casting, Welding and Advanced Solidification Processes VII, ed. M. Cross, J. Campbell (TMS, 1995), 649-656.
5. H.E. Exner, M. Rettenmayer, A. Roosz, "Some components on the present state of micromodels for dendritic solidification" Mat. Sci. Forum 77 (1991), 205-210
6. P.N. Hansen, P.R. Sahm, "Simulation and Modeling for Advanced Solidification Processes", in Proc. of. Int. Conf. Modeling of Casting and Welding Processes IV, ed. A.F. Giamei , G.J. Abbaschian (TMS, 1988), 529-542.
7. M. Fackeldey et al., "Recent Advances in the Application of a Combined Heat, Stress and Microstructure Simulation on the Casting Process of a Single Crystal Turbine Blade", in Proc. of 4th Decennial Int. Conf. On Solidification Processing, Sheffield (1997), 41-44.
8. M. Fackeldey, A. Ludwig, P.R. Sahm: "Coupled Modeling of the Solidification Process Predicting Temperatures, Stresses and Microstructures", Comp. Mater. Sci. 7 (1/2) (1996), 194-199.
9. A. Roósz, E. Halder, H.E. Exner, "Num. Calculation of Microsegregation in Coarsened Dendritic Microstructure", Mater. Sci. Tech. 2 (1986), 1149-1155.
10. A. Roósz, H.E. Exner, "Num. Modelling of Dendritic Solidification in Aluminium-Rich Al-Cu-Mg Alloys", Acta Metall. Mater. 38 (1990), 375-380.
11. A. Roósz, H.E. Exner, "A Complete Model for Microsegregation During Columnar Dendritic Growth", in Proc. of Int. Conf. Modeling of Casting, Welding and Advanced Solidification Processes VI, ed. T.S. Piwonka, V. Voller, L. Katgerman (TMS, 1993), 243-250.
12. T. Kraft, "Numerical Microsegregation Model for Dendritic Solidification: Model Description and Applications", Int. J. Cast Metals, 9 (1996), 51-61.
13. N. Anderson, A. Björck, "A New High Order Method of Regula Falsi Typ for Computing a Root of an Equation", BIT 13 (1973), 253-264.
14. W. Kurz, D.J. Fisher, Fundamental of Solidification, 3th edition (Switzerland, Trans Tech Publ. 1992)
15. R. Sasikumar, H.E Exner, "Coupling of Microsegregation Models to Heat Flow Simulations in Castings", Modeling Simul. Mater. Sci. Eng 1 (1992), 19-27.